

Measuring neutron star mass and radius with three mass–radius relations

C. M. Zhang,^{1*} H. X. Yin,¹ Y. Kojima,² H. K. Chang,³ R. X. Xu,⁴ X. D. Li,⁵ B. Zhang⁶
and B. Kiziltan⁷

¹National Astronomical Observatories, Chinese Academy of Sciences, Beijing 100012, China

²Department of Physics, Hiroshima University, Higashi-Hiroshima 739-8526, Japan

³Department of Physics and Institute of Astronomy, National Tsing Hua University, Hsinchu 30013, Taiwan

⁴Department of Astronomy, Peking University, Beijing 100871, China

⁵Department of Astronomy, Nanjing University, Nanjing 210093, China

⁶Department of Physics, University of Nevada, NV 89154-4002, USA

⁷Department of Astronomy & Astrophysics, University of California, Santa Cruz, USA

Accepted 2006 October 2. Received 2006 August 11; in original form 2005 December 6

ABSTRACT

We propose to determine the mass and radius of a neutron star (NS) using three measurable mass–radius relationships, namely the ‘apparent’ radius inferred from the NS thermal emission, the gravitational redshift inferred from the absorption lines, as well as the averaged stellar mass density inferred from the orbital Keplerian frequency derived from the kilohertz quasi-periodic oscillation data. We apply the method to constrain the NS mass and radius of the X-ray sources, 1E 1207.4–5209, Aql X-1 and EXO 0748–676.

Key words: equation of state – stars: neutron – pulsars: general – X-rays: stars.

1 INTRODUCTION

Measuring the mass (M) and radius (R) of a neutron star (NS) is very important in both nuclear physics and gravitational physics since it allows us to constrain the NS matter compositions (e.g. neutrons or quarks) at superdensity (see e.g. Alcock, Farhi & Olinto 1986; Haensel et al. 1986; Cheng et al. 1998; Li et al. 1999; Miller 2002; Lattimer & Prakash 2004), and to trace the particle motion behaviour in superstrong gravitational field (see e.g. van der Klis 2000, 2006).

NS masses have been measured in the radio pulsar binary systems with high precision (see e.g. Kaspi, Taylor & Ryba 1994; Bailes et al. 2003). For example, the two NS masses of the Hulse–Taylor pulsar system, PSR 1913+16, have been measured as $M = 1.41$ and $1.38 M_{\odot}$, respectively (see e.g. Manchester & Taylor 1977), and those of the recently discovered double pulsar system, PSR J0737–3039, are $M = 1.34$ and $1.25 M_{\odot}$, respectively (see e.g. Lyne et al. 2004). The mass constraints of 26 NSs in the binary radio pulsar systems have been derived by Thorsett & Chakrabarty (1999), who present a remarkably narrow underlying Gaussian mass distribution at $M = 1.35 \pm 0.04 M_{\odot}$. In the low mass X-ray binaries (LMXBs), a lower mass limit $M > 0.97 \pm 0.24 M_{\odot}$ was derived for the NS in 2A 1822–371 (Jonker, van der Klis & Groot 2003), and the NS mass in Cyg X-2 was derived as $M = 1.78 \pm 0.23 M_{\odot}$ (Orosz & Kuulkers 1999).

In contrast, there is no method so far to directly measure the radius of a NS. A conventional value of NS radius is about 15 km,

which is derived by requiring that the averaged dipolar magnetic field strength (i.e. $\sim 10^{12}$ G) inferred from radio pulsar spin-down (see e.g. Manchester & Taylor 1977), is consistent with the one implied by the cyclotron line emission in some X-ray binaries (see e.g. Truemper et al. 1978; Makishima et al. 1999). The uncertainties in determining the NS radius make it difficult to accurately measure the NS equation of state (EOS). The detail of matter composition inside a NS has been an open issue.

With the launches of X-ray space observatories, especially the recent *XMM–Newton*, *Chandra* and *RXTE* (see e.g. van der Klis 2000, 2006; Jansen et al. 2001), some M – R relationships have been appropriately measured or estimated. These include (i) the ‘apparent radius’ R_{∞} estimated from the thermal emission of isolated NSs (e.g. Geminga, Caraveo et al. 2004; 1E 1207.4–5209, Bignami et al. 2004; RX J1856.5–3754, Burwitz et al. 2001, 2003; Truemper et al. 2004) or NSs in binary systems (e.g. Aql X-1, Rutledge et al. 2001); (ii) the gravitational redshift implied from the absorption lines in EXO 0748–676 and 4U 1700+24 (e.g. Cottam, Paerels & Mendez 2002; Tiengo et al. 2005) and (iii) the averaged NS mass density inferred from the orbital Keplerian frequency used to interpret the kilohertz quasi-periodic oscillations (kHz QPOs) discovered by *RXTE* (see e.g. Miller, Lamb & Psaltis 1998; van der Klis 2000, 2006; Zhang 2004).

Generally speaking, if two of the three above M – R relations are well ‘measured’, one can solve both M and R independently. This is the main topic of this paper. We will discuss the methods in detail and apply them to several sources. Once the NS M and R regions are known, we can evaluate the matter compositions inside the star. As shown in the three figures, we have chosen the EOSs of strange matter (CS1 and CS2), normal neutron matter (CN1 and CN2) and

*E-mail: zhangcm@bao.ac.cn

pion condensate in the star core (CPC) (see e.g. Cook, Shapiro & Teukolsky 1994; Lattimer & Prakash 2001).

2 MEASURING NS MASS AND RADIUS WITH M – R RELATIONS

(i) The ‘apparent radius’ R_∞ inferred from the thermal emission data is only an upper limit of the NS radius. It is related to the ‘true’ radius R through (see e.g. Thorne 1977; Haensel 2001; Lattimer & Prakash 2001),

$$R_\infty = R/\sqrt{1 - R_s/R}, \quad (1)$$

where $R_s = 2GM$ is the Schwarzschild radius. From equation (1), the maximum value of the mass can be easily obtained as $M = 1.3(R_\infty/10^6 \text{ cm})M_\odot$ when $R = 0.58 R_\infty$. We stress that the apparent radius is not a directly observable quantity although derivable (in principle) from two observable quantities, namely the ‘apparent blackbody luminosity’ (the blackbody luminosity seen by a distant observer) and the ‘apparent blackbody temperature’. Both quantities are derived by fitting X-ray data under the assumption of perfect blackbody, which is, in general, not true (see Haensel 2001). In particular, the inclusion of an atmosphere above the NS crust can vary the estimate of the NS apparent radius by more than a factor of 2 (see Haensel 2001, section 3.1), thus the ‘measured’ apparent radius is still model-dependent.

(ii) The gravitational redshift near the NS surface provides another M – R relation, giving the ratio between the NS mass and radius (e.g. Miller 2002). The approach becomes relevant with the recent discovery of the absorption features in EXO 0748–676 (Cottam et al. 2002). According to the definition of the gravitational redshift, $z = \Delta\lambda/\lambda \simeq GM/R$ (for a weak gravitational field, where λ is the wavelength of the emission), for a non-rotating spherical gravitational source in Schwarzschild space–time, we get (see e.g. Sanwal et al. 2002)

$$1 + z = 1/\sqrt{1 - R_s/R}, \quad (2)$$

or in terms of M/R ,

$$m/R_6 = f(z) = \frac{z(1 + z/2)}{0.15(1 + z)^2}, \quad (3)$$

where $R_6 = R/10^6 \text{ cm}$, and $m = M/M_\odot$ is the mass in unit of solar mass. In the case of weak gravitational fields ($z \ll 1$), $f(z) \simeq z/0.15$ is approximately obtained.

(iii) A third M – R relation can be obtained by analysing the kHz QPO data. This field has been greatly benefited from the *RXTE* mission, which discovered the twin (upper and lower) kHz QPOs or millisecond variability in the X-ray data of about 20 NS LMXB systems. The upper kHz QPO frequency is generally interpreted as the Keplerian frequency ν_K of orbital materials at some preferred radius r near the NS surface (Stella & Vietri 1999; Morsink 2000; van der Klis 2000, 2006; Zhang 2004), i.e.

$$\nu_K = \sqrt{\frac{GM}{4\pi^2 r^3}} = 1850 \text{ (Hz)} A X^{3/2}, \quad X = R/r, \quad (4)$$

with the parameter $A = (m/R_6^3)^{1/2}$ or $R_6 = 1.27 m^{1/3} (A/0.7)^{-2/3}$, where R_6 is the NS radius in unit of 10 km. The physical meaning of the parameter A is such that the quantity A^2 represents the ‘measurement’ of the averaged NS mass density, namely

$$M/R^3 \simeq 10^{15} \text{ (g cm}^{-3}\text{)} (A/0.7)^2. \quad (5)$$

Meanwhile, by interpreting the twin kHz QPOs as the Keplerian motion and the Alfvén wave oscillation mechanism (see e.g. Zhang

2004), the averaged mass density parameter A can be inferred from the simultaneously detected twin kHz QPO frequencies. For the typical kHz QPO sources, $A \simeq 0.7$ is approximately obtained (Zhang 2004). If, instead, only one single kHz QPO frequency is detected, one cannot derive the exact value of A from the model, but can estimate the lower limit of A and the upper limit of M according to the following arguments, as proposed by Miller et al. (1998). In order to explain the observed X-ray flux saturation at the twin kHz QPO frequencies (e.g. Zhang et al. 1998; van der Klis 2000, 2006), it is usually believed that the maximum Keplerian frequency ν_K occurs either at the star surface ($r = R: X = 1$) or at the innermost stable circular orbit (ISCO) with the radius $R_{\text{ISCO}} = 3R_s = 6GM$. The two inequalities are therefore derived from equation (4) of Miller et al. (1998), i.e.

$$A \geq \nu_K/1850 \text{ (Hz)}, \quad (6)$$

and

$$m \leq 2200 \text{ (Hz)}/\nu_K. \quad (7)$$

In addition, Burderi & King (1998) have derived a M – R relation for the millisecond accretion-powered X-ray pulsar SAX J1808.4–3658 with the measured spin frequency 401 Hz through comparing the stellar radius with its corotation radius of the magnetosphere disc. They inferred a value of $A > 0.62$.

To summarize, hitherto there are roughly three kinds of well-known M – R relationships that could be measured or estimated from the data, as described above. Knowing two of the three in a system would in principle lead to the determination of both M and R . In reality, errors are large for these relationships. Knowing all three relations for a source would greatly diminish the errors. As an illustration, below we will use the method to constrain M and R for several sources.

2.1 Constraining M and R with R_∞ and z : the case of 1E 1207.4–5209

If the ‘apparent radius’ R_∞ and the gravitational redshift z are known, both M and R can be calculated by the following two formulae, derived from equations (1) and (2),

$$R_6 = R_{\infty 6}/(1 + z), \quad (8)$$

$$m = f(z)R_{\infty 6}/(1 + z), \quad (9)$$

with $R_{\infty 6} = R_\infty/10^6 \text{ cm}$.

In the spectral analysis of 1E 1207.4–5209, Bignami et al. (2004) found that the best-fitting continuum model includes two blackbody components, i.e. a cooler component with a temperature $KT = 0.163 \pm 0.003 \text{ keV}$ and an emitting radius of $R_e = 4.6 \pm 0.1 \text{ km}$, and a hotter component with $KT = 0.319 \pm 0.002 \text{ keV}$ and $R_e = 0.83 \pm 0.03 \text{ km}$. If we take the cooler component as the emission from the whole star, then the cooler emitting radius $4.6 \pm 0.1 \text{ km}$ can be regarded as a measured lower limit of the ‘apparent radius’ R_∞ . In addition, an emitting radius $R = 4.6 \pm 0.1 (d/2 \text{ kpc}) \text{ km}$ in 1E 1207.4–5209 is obtained by the best-fitting continuum model of the blackbody function and by the distance of 2 kpc (Bignami et al. 2004), however as claimed by Haensel (2001) that an emitting radius may be doubled if the atmosphere model of the photon spectrum is considered, i.e. the emitting radius may be as high as $\sim 9.4 \text{ km}$.

On the other hand, two absorption features in the spectrum of 1E 1207.4–5209 were detected with the *Chandra* ACIS (Sanwal et al. 2002). Interpreting these lines as helium atomic lines, a gravitational redshift is inferred as $z \sim (0.12\text{--}0.23)$ (Sanwal et al. 2002).

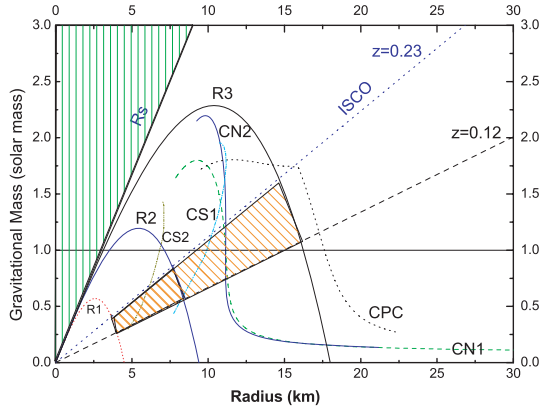


Figure 1. The M – R diagram. Five representative EOSs are shown (see also e.g. Miller 2002): stars containing strange quark matter (CS1 and CS2), stars made of normal neutron matter (CN1 and CN2) and stars with pion condensate cores (CPC) (Cook et al. 1994; Lattimer & Prakash 2001). The straight lines are constant z lines: the solid (R_s) and the dotted lines (ISCO) represent that the radius is one and three times of the Schwarzschild radius, i.e. $R = 2GM$ (below the line R_s , the NS M – R regimes are possible; see e.g. Haensel et al. 1986) and $R = 6GM$, respectively. The constant redshift lines $z = 0.12$ and 0.23 are also plotted. The concave-down parabolas are constant R_∞ lines: $R_\infty = 4.5, 9.4$ and 18 km labelled by R1, R2 and R3 correspond to the lower limit of the apparent radius of 1E 1207.4–5290 ($4.5 = 4.6 - 0.1$) inferred by the blackbody assumption (Bignami et al. 2004) that [$9.4 = 2 \times (4.6 + 0.1)$] estimated by taking into account the factor of 2 uncertainty because of the inclusion of the NS atmosphere (Haensel 2001), and that ($18 = 4.6 \times 2 \times 3.9/2$) by considering the possible longer distance from the source to the Earth $d \sim 3.9$ kpc (see e.g. Pavlov et al. 2004), respectively. The shadowed area stands for the possible M – R range of 1E 1207.4–5209, which covers the EOSs of the strange matter and normal neutrons.

This conclusion is, however, inconclusive, since the lines may be due to the cyclotron origin (e.g. De Luca et al. 2004). Here, we take this gravitational redshift measurement as an unconfirmed, tentative case.

In Fig. 1, we present the NS M – R diagram. For the possible parameter ranges of 1E1207.4–5209, $R_\infty = 4.6 \pm 0.1$ ($d/2$ kpc) and $z = 0.12$ – 0.23 , i.e. $R_\infty = 4.5$ ($= 4.6 - 0.1$) (km) as estimated from the blackbody assumption (Bignami et al. 2004), $R_\infty = 9.4$ [$= (4.6 + 0.1) \times 2$] (km), while the atmosphere model of photon spectrum is taken into account (Haensel 2001), we constrain the M – R region in the shadowed area enclosed by the lines labelled as R1 and R2, and those labelled as $z = 0.12$ and 0.23 , where the inferred M – R regime for 1E 1207.4–5209 favours the existence of the strange matter inside NS. However, it is pointed out by Truemper (private communication) that the distance d from 1E 1207.4–5209 to the Earth is not so certain and $d = 1.3 \sim 3.9$ kpc has been given (see e.g. Pavlov, Sanwal & Teter 2004). If we consider the atmosphere model of photon spectrum and the distance $d = 3.9$ kpc, then the derived ‘apparent radius’ can be as large as 18 km ($18 = 4.6 \times 2 \times 3.9/2$), which will weaken the conclusion of 1E 1207.4–5209 including a strange star because the inferred M – R range in Fig. 1 is enlarged to cover the EOSs of normal neutrons.

Furthermore, if one assumes the validity of the above measured R_∞ (4.5–4.7 km) and z (0.12–0.23), then one gets $M = 0.34 \pm 0.09 M_\odot$ and $R = 4.2 \pm 0.1$ km for 1E 1207.4–5209 according to equations (8) and (9). In this case, one does conclude that the NS EOS of 1E 1207.4–5209 involves in the composition of strange quark matters (e.g. Xu 2005). Apparently, this conclusion is model-dependent and based on the assumptions of blackbody spectrum and the distance of 2 kpc.

In addition, in Fig. 1, we also plot the lines of $R = R_s = 2GM$ (the solid straight line labelled as R_s , below which the M – R values will be permitted for NSs) and $R = R_{\text{ISCO}} = 6GM$ (the middle straight dotted line labelled as ISCO). The latter corresponds to $z = 0.23$ (this value is fortuitous coincidence with the observationally inferred redshift upper limit of 1E 1207.4–5209, see Sanwal et al. 2002) and divides the M – R diagram into the $R < R_{\text{ISCO}}$ region (above the line) and the $R > R_{\text{ISCO}}$ region (below the line).

2.2 Constraining M and R with R_∞ and A : the case of Aql X-1

If the apparent radius R_∞ and the parameter A are known, both M and R can be calculated by the following two formulae, derived from equations (1) and (5),

$$R_6 = R_\infty / \sqrt{1 + 0.15(A/0.7)^2 R_\infty^2}, \quad (10)$$

$$m = 0.49(A/0.7)^2 \left[R_\infty / \sqrt{1 + 0.15(A/0.7)^2 R_\infty^2} \right]^3. \quad (11)$$

The quiescent spectrum of transient type-I X-ray bursting NS Aql X-1 is measured with *Chandra*/ACIS-S, and the best-fitting value of the apparent radius $R_\infty = 13.4^{+5}_{-4}$ ($d/5$ kpc) km is inferred by assuming a pure hydrogen atmosphere with the temperatures ranging from 145 to 168 eV, plus a power-law component. The distance from the observer to source is 5 kpc as a fiducial value because the current uncertainties allow for a distance from 4 to 6.5 kpc (Rutledge et al. 2001). Therefore, including the uncertainty on source distance the lower and upper limits on R_∞ are 7.5 km [$(13.4 - 4) \times 4/5$] and 23.9 km [$(13.4 + 5) \times 6.5/5$], respectively. Moreover, the single kHz QPO frequency 1040 Hz has been detected in Aql X-1 by *RXTE* (e.g. van der Klis 2000, 2006), so that according to equations (6) and (7), one can get the constraints $A \geq 0.56$ and $m \leq 2.1$. In Fig. 2, the ranges of M and R of NS in Aql X-1 are confined in the shadowed area where the meanings of the boundaries are indicated in the figure caption. We find that the shadowed area has a loose constraint on NS EOSs, and it implies all representative EOSs of the strange matter, normal neutrons and pion condensate in star core. Moreover, it is worth noting that the $A = 1.0$ parabola divides the M – R diagram into two parts (Fig. 2), and the strange star EOSs are relevant only when $A > 1.0$.

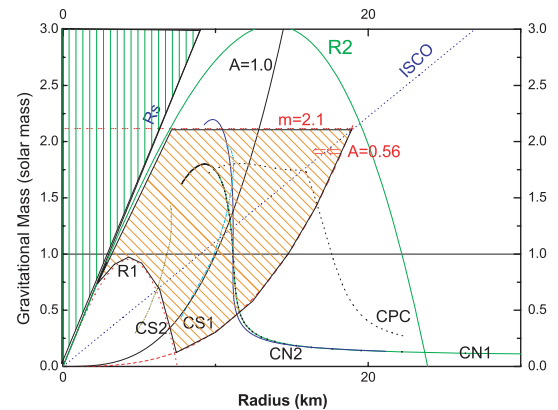


Figure 2. Same as Fig. 1. The mass and radius of NS in Aql X-1 are constrained in the shaded area. R1 (R2) represents $R_\infty = 7.5$ (23.9) (km), where the lower and upper limits of R_∞ on account of the uncertainty by the source distance are 7.5 km [$(13.4 - 4) \times 4/5$] and 23.9 km [$(13.4 + 5) \times 6.5/5$], respectively. The two concave-up parabolas stand for $A = 0.56$ and 1.0 , respectively (as marked). The horizontal line $m = 2.1$ represents $M = 2.1 M_\odot$.

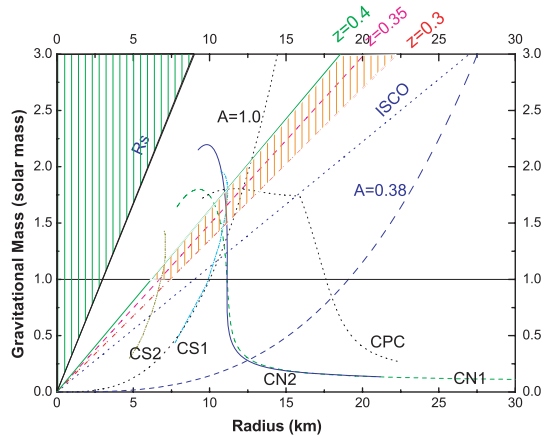


Figure 3. Same as Figs 1 and 2. The mass and radius of the NS in EXO 0748–676 are constrained by the line $z = 0.35$ and two horizontal lines representing one (three) solar mass(es). Cottam et al. (2002) declaimed the gravitational redshift $z = 0.35$ with a small error, but this small error is not given quantitatively. As a possible contrast in case of the error, we plot the lines with redshifts $z = 0.3$ and 0.4 .

2.3 Constraining M and R with A and z : the case of EXO 0748–676

If the gravitational redshift z and the parameter A are known, both M and R can be calculated by the following two formulae, derived from equations (2) and (5),

$$R_6 = 1.43 f^{1/2}(z)(A/0.7)^{-1}, \quad (12)$$

$$m = 1.43 f^{3/2}(z)(A/0.7)^{-1}. \quad (13)$$

In the case that only a single kHz QPO frequency is detected, we can place a lower limit on the parameter A from equation (6). Following equations (12) and (13), M and R are constrained by the following inequalities

$$R_6 \leq [1850(\text{Hz})/\nu_K] f^{1/2}(z), \quad (14)$$

$$m \leq [1850(\text{Hz})/\nu_K] f^{3/2}(z). \quad (15)$$

A gravitational redshift $z = 0.35$ was detected in EXO 0748–676 by Cottam et al. (2002), who identify the most significant features with the Fe xxvi and xxv $n = 2-3$ and O VIII $n = 1-2$ transitions, all with a redshift of $z = 0.35$, identical within small uncertainties for the respective transitions, however, this small error has not been given quantitatively by the authors. In order to present the possible influence of the redshift variation on the M – R region, we plot $z = 0.3$ and 0.4 lines in Fig. 3. Furthermore, a single kHz QPO frequency 695 Hz is detected by *RXTE* for the same source (e.g. Homan & van der Klis 2000; van der Klis 2000). Thus, $A \geq 0.38$ and $m \leq 3.2$ are inferred from equations (6) and (7). As shown in Fig. 3, the $A \geq 0.38$ condition gives a very loose constraint, which has little help to constrain the NS mass into a domain of less than $3 M_\odot$ because the detected QPO frequency of this source is abnormally lower than the typical values 1000 Hz (see van der Klis 2000, 2006). If the future detections of this source present the higher frequency, then the promising constrain condition would be improved. Moreover, since $M = 0.97 \pm 0.24 M_\odot$ was measured as a lower mass for 2A 1822–371 (Jonker et al. 2003), we set 1.0 and $3.0 M_\odot$ as the conservative lower and upper mass limits for NSs, respectively. The M – R constraint for EXO 0748–676 is then limited to the segment of the straight dashed line $z = 0.35$ between

the two horizontal lines $m = 1.0$ and 3.0 , where the EOSs for the strange matter, normal neutron and pion condensate in star core are all permitted.

3 SUMMARY AND DISCUSSION

In this paper, we discuss the possibility of using any two of the three M – R relationships to constrain NS mass and radius. The three M – R relationships include the ‘apparent radius’ (R_∞), the gravitational redshift (z) and the averaged mass density (A^2). We applied the method to three sample sources, 1E 1207.4–5209, Aql X-1 and EXO 0748–676. In principle, if all the above three M – R relations are well measured in one source, one can pose tight constraints on the ranges of M and R , so that the potential NS EOSs would be inferred. Unfortunately, this is not achieved so far. Furthermore, some M – R relations are incomplete or have large errors, so that additional astrophysical arguments are needed, and one can derive some inferred lower or upper limits of the M – R relations (e.g. equations 6 and 7). In binary systems, if the NS mass is known, any one of the three M – R relation measurements would be sufficient to derive its radius.

For the compact star in 1E 1207.4–5209, the estimates of its mass and radius come from the possible lower limit of the calculated apparent radius of about 4.6 km (Bignami et al. 2004). An extraordinary low mass is inferred, which is even less than the measured lower limit of NS mass $0.97 \pm 0.24 M_\odot$ in 2A 1822–371 (Jonker et al. 2003). In such a case, the existence of exotic matter inside the star is hinted under the assumptions of blackbody spectrum and 2-kpc distance.

The stellar radius can be also estimated by the motion-induced Doppler broadening of absorption lines, when the emission region moves towards and away from the observer as the star rotates. According to this, Villarreal & Strohmayer (2004) have studied the source EXO 0748–676 with the measured gravitational redshift $z = 0.35$ (Cottam et al. 2002), and obtained a radius of about 11.5 km and a stellar mass of about $1.75 M_\odot$. A remark is that the emission latitude and the orientation of the rotation axis both affect the result, so that the method is model-dependent.

In addition, from the recent further study, Chang et al. (2005) show that the intrinsically broad-line profile prohibits any meaningful constraint on the NS radius if the 45-Hz burst oscillation seen by Villarreal & Strohmayer (2004) is the spin frequency.

It is worth mentioning that the measured apparent radius of isolated NS in RX J1856.5–3754, because of the distance of this source to Earth, is well determined to be about 117 pc (see e.g. Walter & Lattimer 2002); with the perfect blackbody spectrum of this source (Burwitz et al. 2001, 2003; Drake et al. 2002) the conservative lower limit of apparent radius has been implied to be 16.5 km ($d/117$ pc) (Truemper et al. 2004). This corresponds to the ‘true’ radius of 14 km for a $1.4 M_\odot$ NS, indicating a stiff EOS at high densities, which excludes the quark stars or even the NSs with the quark cores (Truemper et al. 2004). Moreover, without knowledge of the spectrum line in RX J1856.5–3754 until now (see e.g. Drake et al. 2002), we cannot constrain its M and R independently (Truemper, private communication). Once again, it is noted that the above conclusion comes from the blackbody spectrum assumption, and the apparent radius may confront a modification by more than a factor of 2 if using the atmosphere model of photon spectrum (Haensel 2001).

The next generation X-ray observatories with enhanced spectral and timing capabilities would greatly improve the ‘measurements’ of the three M – R relations discussed in this paper. This would strengthen our confidence in evaluating the superdense

nuclear compositions of compact stars. Theoretically, if both M and R of a compact star are accurately measured, its EOS and nuclear matter compositions would be explicitly revealed. This in turn sheds light on the unknown astrophysical processes during the supernova explosion of its progenitor star (e.g. Podsiadlowski et al. 2005). On the other hand, the regime of non-Newtonian strong gravitational fields would be also revealed with the determination of the NS mass and radius, where the direct tests of Einstein's theory of general relativity will be possible in the near future (e.g. van der Klis 2000, 2006).

ACKNOWLEDGMENTS

We are grateful to M. C. Miller for providing the EOS data files. Thanks are also due to the helpful discussions with V. Burwitz, J. Truemper, J. M. Lattimer, K. S. Cheng, Z. G. Dai, T. Lu, D. M. Wei, Z. R. Wang, Q. H. Peng, J. L. Han, G. J. Qiao and X. J. Wu. We specially thank J. Truemper for many suggestions and advice, and for initializing discussions on M - R relation of RX J1856.5-3754. This research has been supported by the innovative project of CAS of China. We are very grateful to the anonymous referee for critic comments that greatly improve the quality of the paper.

REFERENCES

- Alcock C., Farhi E., Olinto A., 1986, *Phys. Rev. Lett.*, 57, 2088
 Bailes M., Ord S. M., Knight H. S., Hotan A. W., 2003, *ApJ*, 595, L49
 Bignami G. F., De Luca A., Caraveo P. A., Mereghetti S., Moroni M., Mignani R. P., 2004, *Mem. Soc. Astron. Ital.*, 75, 448
 Burderi L., King A. R., 1998, *ApJ*, 505, L135
 Burwitz V., Zavlin V. E., Neuhaeuser R., Predehl P., Truemper J., Brinkman A. C., 2001, *A&A*, 379, L35
 Burwitz V., Haberl F., Neuhaeuser R., Predehl P., Truemper J., Zavlin V. E., 2003, *A&A*, 399, 1109
 Caraveo P. A., De Luca A., Mereghetti S., Pellizzoni A., Bignami G. F., 2004, *Sci*, 305, 376
 Chang P., Morsink M., Bildsten L., Wasserman I., 2005, *ApJ*, 636, L117
 Cheng K. S., Dai Z. G., Wei D. M., Lu T., 1998, *Sci*, 280, 407
 Cook G. B., Shapiro S. L., Teukolsky S. A., 1994, *ApJ*, 424, 823
 Cottam J., Paerels F., Mendez M., 2002, *Nat*, 420, 51
 De Luca A., Mereghetti S., Caraveo P. A., Moroni M., Mignani R. P., Bignami G. F., 2004, *A&A*, 418, 625
 Drake J. J. et al., 2002, *ApJ*, 572, 996
 Haensel P., 2001, *A&A*, 380, 186
 Haensel P., Zdunik J. L., Schaefer R., 1986, *A&A*, 160, 121
 Homan J., van der Klis M., 2000, *ApJ*, 539, 847
 Jansen F. et al., 2001, *A&A*, 365, L1
 Jonker P. G., van der Klis M., Groot P. J., 2003, *MNRAS*, 339, 663
 Kaspi V., Taylor J., Ryba M., 1994, *ApJ*, 428, 713
 Lattimer J. M., Prakash M., 2001, *ApJ*, 550, L426
 Lattimer J. M., Prakash M., 2004, *Sci*, 304, 536
 Li X. D., Bombaci I., Dey M., Dey J., van den Heuvel E. P. J., 1999, *Phys. Rev. Lett.*, 3776, 83
 Lyne A. G. et al., 2004, *Sci*, 303, 1089
 Makishima K., Mihara T., Nagase F., Tanaka Y., 1999, *ApJ*, 525, 978
 Manchester R. N., Taylor J. H., 1977, *Pulsars*. Freeman & Co., San Francisco
 Miller M. C., 2002, *Nat*, 420, 31
 Miller M. C., Lamb F. K., Psaltis D., 1998, *ApJ*, 508, 791
 Morsink S., 2000, *Sci*, 290, 945
 Orosz J. A., Kuulkers E., 1999, *MNRAS*, 305, 1320
 Pavlov G. G., Sanwal D., Teter M. A., 2004, in Camilo F., Gaensler B. M., eds, *Proc. IAU Symp. 218, Young Neutron Stars and Their Environments*. Astron. Soc. Pac., San Francisco, p. 239
 Podsiadlowski P., Dewi J. D., Lesaffre P., Miller J. C., Newton W. G., Stone J. R., 2005, *MNRAS*, 361, 1243
 Rutledge R. E., Bildsten L., Brown E. F., Pavlov G. G., Zavlin V. E., 2001, *ApJ*, 559, 1054
 Sanwal D., Pavlov G. G., Zavlin V. E., Teter M. A., 2002, *ApJ*, 574, L61
 Stella L., Vietri M., 1999, *Phys. Rev. Lett.*, 82, 17
 Thorne K. S., 1977, *ApJ*, 212, 825
 Thorsett S. E., Chakrabarty D., 1999, *ApJ*, 512, 288
 Tiengo A., Galloway D. K., di Salvo T., Mendez M., Miller J. M., Sokolowski J. L., van der Klis M., 2005, *A&A*, 441, 283
 Truemper J. E. et al., 1978, *ApJ*, 219, L105
 Truemper J. E., Burwitz V., Haberl F., Zavlin V. E., 2004, *Nucl. Phys.*, 132, 156
 van der Klis M., 2000, *ARA&A*, 38, 717
 van der Klis M., 2006, in Lewin W. H. G., van der Klis M., eds, *Compact Stellar X-Ray Sources*. Cambridge Univ. Press, Cambridge, p. 39
 Villarreal A. R., Strohmayer T. E., 2004, *ApJ*, 614, L121
 Walter F. M., Lattimer J., 2002, *ApJ*, 576, L145
 Xu R. X., 2005, *MNRAS*, 356, 359
 Zhang C. M., 2004, *A&A*, 423, 401
 Zhang W., Smale A. P., Strohmayer T. E., Swank J. H., 1998, *ApJ*, 500, L171

This paper has been typeset from a $\text{\TeX}/\text{\LaTeX}$ file prepared by the author.